



Cite this: *Analyst*, 2020, **145**, 4569

## A liquid-crystal-based immunosensor for the detection of cardiac troponin I

Chunli Xia,<sup>a</sup> Dong Zhou,<sup>a</sup> Yueming Su,<sup>a</sup> Guangkai Zhou,<sup>b</sup> Lishuang Yao,<sup>c,d</sup> Weimin Sun<sup>a</sup> and Yongjun Liu<sup>\*a,c</sup>

Cardiac troponin I (cTnI) is one of the most sensitive and specific markers of myocardial cell injury, which can detect even minor myocardial damages. It is recognized as the main biochemical marker of the rapid diagnosis of acute myocardial infarction (AMI) and acute coronary syndrome (ACS). In this study, a label-free biosensor that utilizes the birefringence property of a nematic liquid crystal (LC) for the detection of cTnI is demonstrated. A chemically sensitive film with specific molecular recognition ability was decorated on the surface of a substrate, and the LC molecules were arranged in a vertically oriented order under the influence of the sensitive film, and a dark background signal was obtained using a polarizing optical microscope. When the antigen–antibody specifically binds to form a stronger acting force, the orientation of the LC molecules changes, resulting in a bright optical appearance. This LC-based immunosensor not only has the advantages of a facile structure, low cost and excellent specificity but also high sensitivity (a low detection limit of 1 pg mL<sup>-1</sup>), and has a promising future in biomedical related fields.

Received 1st March 2020,  
Accepted 2nd May 2020

DOI: 10.1039/d0an00425a

rsc.li/analyst

### 1. Introduction

Cardiac troponin I (cTnI) is a type of regulatory protein peculiar to the myocardial tissue, which inhibits the binding of myosin to actin and plays an important role in myocardial contraction.<sup>1–3</sup> A large number of studies have shown that the cTnI level rises instantly with high amplitude variation in the early acute myocardial infarction (AMI) and has high sensitivity. In addition, cTnI possesses a high cardiomyocyte specificity that is not functioned in any type of skeletal muscle.<sup>4–6</sup> The specificity of cTnI for the diagnosis of myocardial infarction (MI) is 96%, and the sensitivity is 97%.<sup>7–9</sup> Therefore, cTnI is one of the most sensitive and specific serum markers of myocardial cell injury.<sup>10,11</sup> Moreover, cTnI has the advantages of definite diagnostic threshold and rapid detection,<sup>12,13</sup> and has gradually become the main biochemical indicator for judging myocardial cell injury in AMI patients.<sup>14,15</sup>

At present, several methods, such as the enzyme-linked immunosorbent assay (ELISA),<sup>16,17</sup> fluorescence immunoassay,<sup>18</sup> colorimetry,<sup>19</sup> electrochemistry,<sup>20</sup> paramagnetic<sup>21</sup> and

surface plasma resonance (SPR),<sup>22</sup> have been studied to monitor the cTnI levels. These methods have specificity for cTnI and play an essential role in detecting cardiac biomarkers. However, there are some obvious shortcomings in these traditional methods, such as the need for complicated instruments and cumbersome detection steps. Furthermore, complex and professional labeling processes require a long time and extra cost. Recently, Liu *et al.*<sup>23</sup> reported a compact biosensor for detecting cTnI based on a phase-shifted microfiber Bragg grating probe. Sandil *et al.*<sup>24</sup> demonstrated a bio-functionalized tungsten trioxide-reduced graphene oxide nanocomposite for the sensitive electrochemical immunosensing of cTnI. Nevertheless, we found that whether it uses microfiber Bragg grating or nanocomposites for sensing, and it was not easy to manufacture the sensing structure, and the production requirements were relatively high. As a result, it was of paramount importance to establish a fast, sensitive, low-cost, and label-free method to detect cTnI.

As a material with numerous excellent properties, liquid crystal (LC) has become a research hot spot. As a special material form between disordered liquid and solid crystal, it possesses the orderliness and optical anisotropy of a crystal molecular arrangement.<sup>25,26</sup> The orientation of the LC molecules is highly sensitive to surface molecular binding events, and the binding of molecules to the surface would induce a change in the LC optical image, which provides a possibility for the sensitive detection of biomolecules<sup>27,28</sup> or chemical reactions.<sup>29</sup> The LC biosensor utilizes the birefringence characteristics of the LC on the polarized light to monitor the change of

<sup>a</sup>Key Lab of In-fiber Integrated Optics, Ministry Education of China, Harbin Engineering University, Harbin 150001, China. E-mail: liuyj@hrbeu.edu.cn

<sup>b</sup>Department of head and neck surgery, Affiliated Tumor Hospital of Harbin Medical University, Harbin 150001, China

<sup>c</sup>State Key Laboratory of Applied Optics, Changchun Institute of Optics, Fine Mechanics and Physics, Chinese Academy of Sciences, Changchun 130033, China

<sup>d</sup>Department of Physics, College of Science, Shantou University, Shantou, 515063, China

the LC orientation caused by a biomolecule, thereby causing a change in the polarization signal. This change can be observed with the naked eye and does not require other expensive and high-end instruments. As a label-free sensor, the LC-based biosensor possesses a simple structure, easy operation, outstanding portability, no need for a special light source and point-of-care (POC) diagnosis. It turns out that the LC-based biosensor has great potential for the detection of the cardiac biomarkers of myocardial infarction. Over the past decades, LC sensors have been applied in the domain of chemical and biological sensing systems.<sup>30,31</sup> However, the methods most researchers used almost utilize one-sided sensing, which limits its sensing effect to some extent, and we believe that the effective use of the other side to sense simultaneously can improve its detection efficiency and further increase its detection sensitivity.

In this study, a new immunosensor based on an LC cell for the sensitive detection of cTnI is reported. Based on a one-sided sensing LC cell method, a double-sided sensing LC cell biosensor was proposed. When LC molecules were vertically oriented with the function of a surfactant, the all-black appearance was observed under a polarizing optical microscope (POM), and the interaction between cTnI and its corresponding antibody may have disturbed the perpendicular alignment of the LC molecules. The sensor shows a fast optical response to the orientation change of the LC, occurring on the surface, and a random optical texture of the surface could be observed using a POM. This new simple LC-based biosensor exhibits high specificity for cTnI compared to other proteins, and its detection sensitivity is also very high, which has a promising prospect in biomolecular detection.

## 2. Experimental section

### 2.1. Materials

Nematic liquid crystal 4-cyano-4'-pentylbiphenyl (5CB) was purchased from Beijing Bayi Space LCD Technology Co., Ltd, China. *N,N*-Dimethyl-*N*-octadecyl (3-aminopropyl) trimethoxysilyl chloride (DMOAP) was purchased from Sigma-Aldrich. Cardiac troponin I antigen was bought from Wondfo Bio-Technology Co., Ltd. Phosphate-buffered saline (PBS), (3-aminopropyl) triethoxysilane (APTES), glutaraldehyde (GA) solution and glycine were obtained from Beijing Innochem Technology Co., Ltd. Cardiac troponin I antibody was purchased from Hytest Bio-Technology Co., Ltd. Human Immunoglobulin G (IgG) and human serum albumin (ALB) were bought from Beijing Bioss Bio-Technology Co., Ltd. Deionized (DI) water was from a Milli-Q system from Millipore, USA, and used in the subsequent experiment.

### 2.2. Pretreatment of glass slides

The slides were cut into 2 cm × 1 cm first, and then soaked in the newly prepared Piranha solution (70% H<sub>2</sub>SO<sub>4</sub> and 30% H<sub>2</sub>O<sub>2</sub>; Notice: Piranha solution has strong oxidizing property and can react drastically with organic matters, and do not store it in a closed container) at 80 °C for 1 h. Next, the slides

were rinsed with absolute ethanol and a large amount of DI water, blown dry with nitrogen and placed in an oven at 110 °C for at least 3 h.

### 2.3. Silylation of glass slides

The slides were decorated by a mixture of solution 1% (v/v) APTES and 1% (v/v) DMOAP, whereby they have soaked in the mixed solution at 80 °C for 1 h (turning them over 30 minutes later). After the reaction has completed, the slides were rinsed with absolute ethanol and plenty of DI water. Finally, the slides were heated in an oven at 110 °C for 1 h after drying under a stream of nitrogen gas.

### 2.4. Coupling of GA

The slides decorated with the APTES/DMOAP self-assembled film were immersed in a 2% GA solution (v/v) and reacted for 1 hour at room temperature. After the reaction was completed, the slides were washed with a large amount of DI water and dried under a stream of nitrogen gas.

### 2.5. Immobilization of cTnI antibody

The slides were then incubated with a cTnI antibody solution (1 μg ml<sup>-1</sup>) in PBS for 2 hours at room temperature and then washed with plenty of water after the incubation. Subsequently, the slides assembled with the anti-cTnI were soaked in a glycine solution (80 mM) at room temperature for 1 h with the purpose of blocking any unreacted aldehyde groups. Finally, the slides were rinsed with DI water and then dried with a small stream of nitrogen gas.

### 2.6. Detection of cTnI and fabrication of LC cells

A cTnI solution in PBS was incubated on the anti-cTnI immobilized surfaces at 37 °C. After 1 h of incubation, the slides were sequentially rinsed with DI water and dried under a stream of gaseous nitrogen. LC optical cells were fabricated by pairing the deposited bottom slide with deposited top glass slide with two thin polyester films as a spacer (thickness is approximately 12 μm) on the left and right sides. 5CB was heated to its isotropic phase (above 35.3 °C) and loaded into an empty space between the two slides using the capillary force. When cooled to room temperature, the liquid crystals are nematic (5CB is nematic at 12 °C–35.3 °C); meanwhile, the enthalpy of the LC phase transition is 17.15 kJ mol<sup>-1</sup>.

### 2.7. Examination of optical images

A POM (CX31 Olympus, Japan) was utilized to examine all the optical images of LC cells. All POM images under cross polarizers were obtained using a CCD camera (DP21, Olympus, Japan) at room temperature.

## 3. Results and discussion

### 3.1. Sensing strategy for the detection of cTnI

The sensing strategy of the proposed LC-based immunosensor is illustrated in Fig. 1. First, a chemically sensitive membrane consisting of a mixture of DMOAP/APTES was assembled on

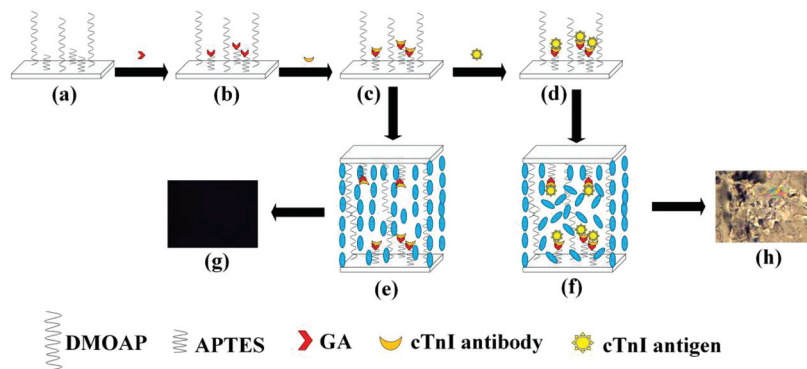


Fig. 1 Schematic of the proposed sensor and sensing strategy.

the surface of the slide (Fig. 1a), which induced the homeotropic alignment of LC molecules. Then, the cTnI antibody was immobilized on the surface of the glass substrate by using the bifunctional cross-linking agent GA (Fig. 1b and c). The LC molecules adopted a homeotropic orientation on the slide when rationally controlling the DMOAP/APTES ratio and the amounts of cTnI antibody immobilized on the slide (Fig. 1e) and thus the image under POM appeared uniformly dark (Fig. 1g). When the cTnI antibody immobilized on a substrate specifically reacted with the cTnI antigen (Fig. 1d), it can disturb the homeotropic alignment of the LC molecules (Fig. 1f), thereby generating different optical response signals (Fig. 1h). The higher the concentration of the specific molecule cTnI, the greater the disturbance and the brighter the optical image, so as to realize the detection of specific biomolecules cTnI. This change of orientation can be detected by a POM on account of the birefringence of LC molecules to polarized light, and this change is directly observed by the naked eye.

### 3.2. Optimization of APTES/DMOAP/GA ratio

The main component of the LC-based biosensor is an LC cell. We initially selected the APTES containing the amino func-

tional group at the end to assemble because the biomolecule can be bonded to APTES by the bifunctional cross-linking agent GA. However, APTES is a silane reagent with a short carbon chain. If the slides are assembled only with it, it cannot effectively induce the homeotropic alignment of LC molecules. In order to achieve the purpose of obtaining a dark background and fixing biomolecules on the slide, we used a mixed solution of APTES/DMOAP to assemble the slides.

As shown in Fig. 2, the ratio of APTES/DMOAP was related to the background brightness value. The images under POM showed a bright-to-dark change with the decrease in the APTES/DMOAP ratio. When the ratio of APTES/DMOAP was 1 : 1 (v/v) or lower, a completely dark stable background was observed, indicating that the LC molecules exhibited a uniform vertical orientation (Fig. 2c). The results showed that the presence of a small amount of APTES does not disturb the vertical alignment of the LC in the cell. In Fig. 2b, a dark texture with some bright spots was observed in a ratio of 5 : 1 (v/v) for the APTES/DMOAP solution. In addition, more bright spots were observed when the APTES/DMOAP volume ratio was 10 : 1 (v/v) (Fig. 2a). In order to obtain sufficient dark background signal and a good self-assembly efficiency of anti-cTnI,

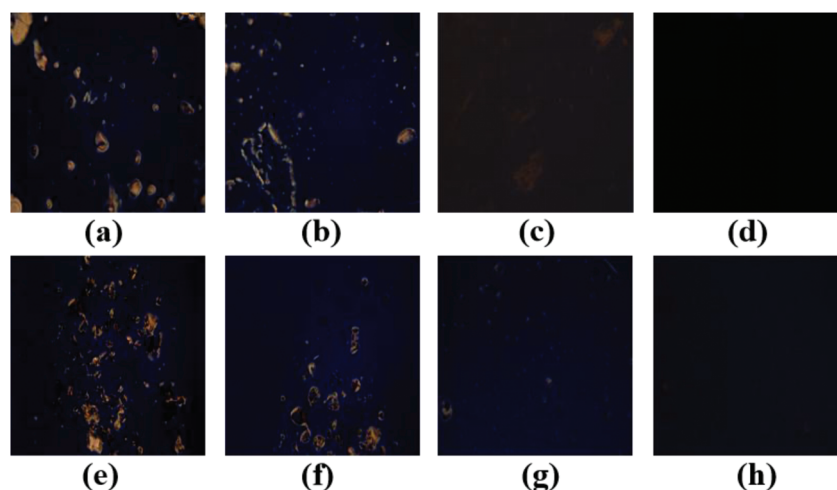


Fig. 2 POM images of LC cells with 5CB in different ratios of DMOAP/APTES. The ratio of APTES/DMOAP was: (a) 10 : 1; (b) 5 : 1; (c) 1 : 1; (d) 0.5 : 1, respectively. Also, after incubation with different ratios of GA (DMOAP/APTES = 1 : 1): (e) 10%; (f) 5%; (g) 2%; (h) 1%.

a 1 : 1 (v/v) APTES/DMOAP ratio was chosen to immobilize the GA.

The background signal was also affected by the amount of GA. Optimization experiments were carried out at different concentrations of GA, and the results are shown in Fig. 2. We found that the optical appearance of the LC cell showed a uniform black image at a concentration of GA of 1% and 2% (Fig. 2h and g). In contrast, when the concentration of GA reached 5% (Fig. 2f) or 10% (Fig. 2e), the LC molecules alignment was disturbed, and some bright spots appeared in the POM image. To ensure maximally immobilized anti-cTnI and a dark background signal, 2% GA was used in subsequent experiments.

### 3.3. Effect of anti-cTnI concentration

The orientation of LC molecules was also closely connected with the concentration of assembled anti-cTnI. In order to

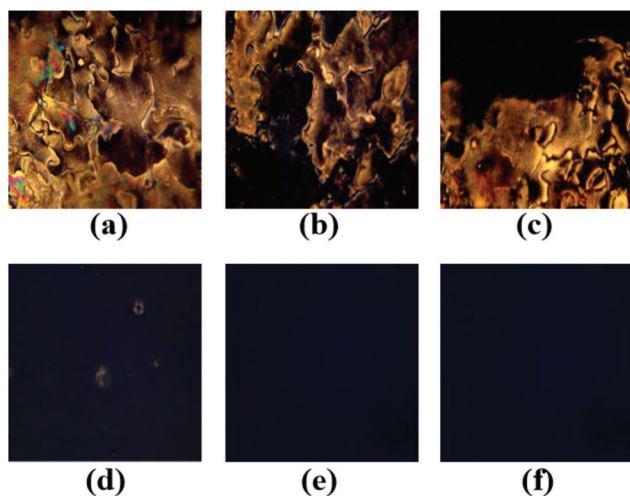


Fig. 3 POM images of LC cells with 5CB after the immobilization with different concentrations of anti-cTnI: (a)  $1000 \mu\text{g ml}^{-1}$ ; (b)  $100 \mu\text{g ml}^{-1}$ ; (c)  $10 \mu\text{g ml}^{-1}$ ; (d)  $1 \mu\text{g ml}^{-1}$ ; (e)  $0.1 \mu\text{g ml}^{-1}$ ; (f)  $0.01 \mu\text{g ml}^{-1}$ .

obtain the optimal concentration of anti-cTnI, we explored several different concentrations of anti-cTnI. As shown in Fig. 3, when the concentration of the anti-cTnI was  $10 \mu\text{g ml}^{-1}$  or higher, a bright large area was observed, indicating that the alignment of LC molecules was disturbed to a large extent by the immobilized anti-cTnI. An almost black optical image was observed when the concentration was equal to or less than  $1 \mu\text{g ml}^{-1}$ , indicating that the LC molecules were arranged neatly. In order to provide as many active groups as possible on the slide substrate and increase the sensitivity of subsequent detection, the anti-cTnI concentration was selected as  $1 \mu\text{g ml}^{-1}$ .

### 3.4. The detection of cTnI

Under the optimal experimental conditions, we examined the detection characteristics of cTnI in the LC biosensor. We initially used the one-sided sensing of the LC cell to detect cTnI. Specifically, the top slide was treated with only 0.5% DMOAP, while the bottom slide was treated to specifically bind the biomolecule for detection. The results are shown in Fig. 4. As the antigen cTnI concentration increases, the intensity and extent of the damage increase gradually, presenting a bright texture under POM. This result indicates that the antigen-antibody binding was stronger than the effect of the vertical surfactant DMOAP on the LC molecules. As the concentration gradually decreases to  $0.1 \text{ ng ml}^{-1}$ , the bright area was already very small, and when the antigen concentration was further lowered, only some bright spots or even all-black images were observed. It indicates that too little antigen was bound, and it cannot disturb the vertical orientation of the LC molecules.

For one-sided sensing LC cell, only one slide is utilized to bind specific molecules. We conjectured that double-sided sensing would be more efficient. Thus, we further explored the sensing of the double-sided liquid crystal cell. As shown in Fig. 5, the addition of cTnI can largely change the optical response and orientation of LC. When the concentration was  $0.001 \text{ ng ml}^{-1}$ , some bright spots were observed. When the concentration was higher, a brighter appearance of the LC cell

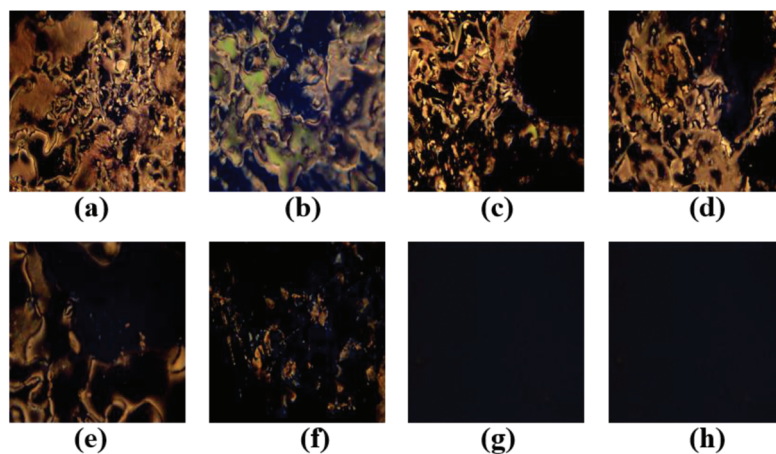
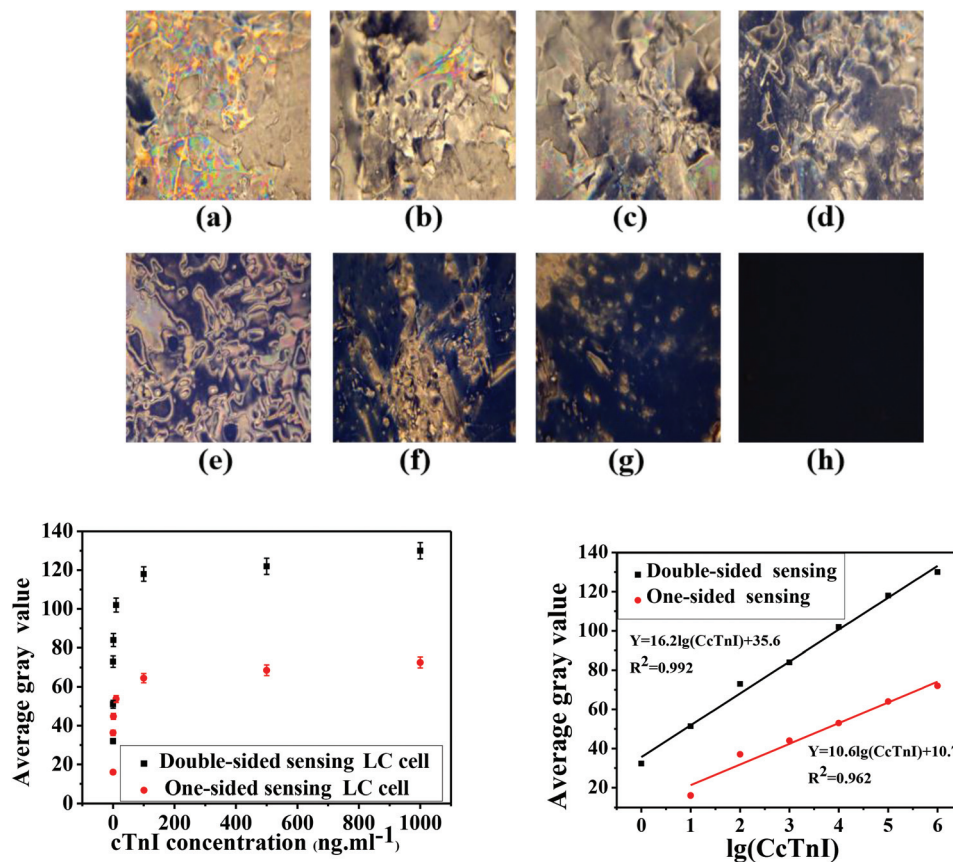


Fig. 4 POM images of LC cells with 5CB with different concentrations of cTnI through the one-sided sensing LC cell: (a)  $1000 \text{ ng ml}^{-1}$ ; (b)  $100 \text{ ng ml}^{-1}$ ; (c)  $10 \text{ ng ml}^{-1}$ ; (d)  $1 \text{ ng ml}^{-1}$ ; (e)  $0.1 \text{ ng ml}^{-1}$ ; (f)  $0.01 \text{ ng ml}^{-1}$ ; (g)  $0.001 \text{ ng ml}^{-1}$ ; (h)  $0.0001 \text{ ng ml}^{-1}$ .



**Fig. 5** POM images of LC cells with 5CB with different concentrations of cTnI through double-sided sensing: (a) 1000 ng ml<sup>-1</sup>; (b) 100 ng ml<sup>-1</sup>; (c) 10 ng ml<sup>-1</sup>; (d) 1 ng ml<sup>-1</sup>; (e) 0.1 ng ml<sup>-1</sup>; (f) 0.01 ng ml<sup>-1</sup>; (g) 0.001 ng ml<sup>-1</sup>; (h) 0.0001 ng ml<sup>-1</sup>. The graph on the left is the relational graph between the average gray value of the image and the cTnI concentration ( $10^1$ – $10^6$  pg ml<sup>-1</sup> for the one-sided sensing LC cell method and  $10^0$ – $10^6$  pg ml<sup>-1</sup> for the double-sided sensing LC cell method), and the right one is a liner fitting between the logarithm of the cTnI concentration ( $10^1$ – $10^6$  pg ml<sup>-1</sup> for the one-sided sensing LC cell method and  $10^0$ – $10^6$  pg ml<sup>-1</sup> for the double-sided sensing LC cell method) and the average gray level of the POM images.

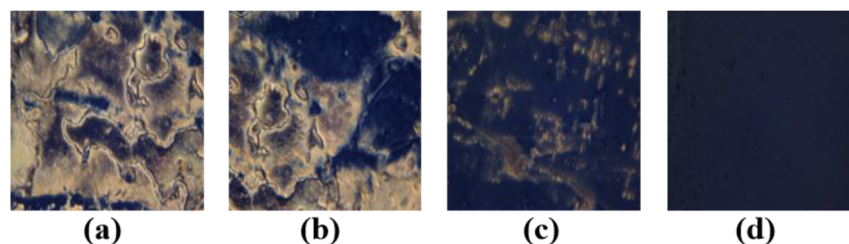
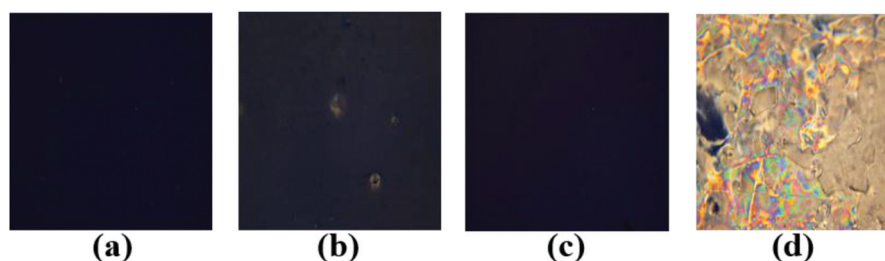
can be observed. We found that the optical appearance of double-sided sensing was different from that of the previous one-sided sensing LC cell sensor. On the one hand, the brightness of double-sided sensing was greater at the same concentration. On the other hand, the detection limit of double-sided was lower and the sensitivity was improved by at least one order of magnitude. Thus, we measured the gray value of the POM images through two sensing methods, respectively, and explored their respective relationship between the cTnI concentration and the gray level of its corresponding POM images. As clearly shown in the left graph of Fig. 5, as the concentration of cTnI increases, the average gray value of the images increased accordingly for both methods. When it increases to a certain value, the gray value changes tend to be gentle because the bound antigen is already close to a saturation value. Besides, as we expected, at the same concentration, its gray value was indeed much higher than the one-sided sensing LC cell detection method. Then, we took the logarithm of the cTnI concentration and found that it had a good linear relationship with the average gray level of the POM image, and the linearity reaches 0.992 for the double-sided sensing LC cell

detection, as shown in the right graph of Fig. 5. However, the linearity reaches 0.962 for one-sided sensing LC cell detection. Through analysis, our proposed double-sided sensing LC cell was superior to the previous one-sided sensing LC cell. Moreover, based on Fig. 5, the limit of detection (LOD) for cTnI was determined to be 1 pg ml<sup>-1</sup>, which is competitive to the existing assays (Table 1).

In order to confirm that the LC molecular perturbation was caused by antibody antigen-specific binding, we performed a series of control experiments in the absence of antibodies, whereby only the antigen was added in various concentrations, as shown in Fig. 6. We observed an almost all-black image when cTnI concentration was 0.01 mg ml<sup>-1</sup>, and complete black background images were obtained when it's below that value. However, it turned out that this concentration value was many times higher than the concentration we detected before, so the influence of antigen can be completely excluded, and the cTnI antigen cannot function alone at low concentrations when anti-cTnI wasn't added. Therefore, the change in the alignment of the LC molecules of the LC cell was due to the specific binding of the anti-cTnI and cTnI.

**Table 1** Comparison of the cTnI biosensors

Detection method	Strategy	LOD	Ref.
ELISA	Cross-flow chromatography	0.027 ng ml <sup>-1</sup>	17
Colorimetry	Au nanoparticles composite	0.01 ng ml <sup>-1</sup>	19
Electrochemistry	Electrochemical impedance spectroscopy	0.11 μg ml <sup>-1</sup>	20
Paramagnetic	Paramagnetic particle	0.5 ng ml <sup>-1</sup>	21
SPR	Resonant circuit	1.4 ng ml <sup>-1</sup>	22
Phase-shifted microfiber Bragg grating	Notch signal	0.03 ng ml <sup>-1</sup>	23
Tungsten trioxide-reduced graphene oxide nanocomposite	Differential pulse voltammetry	0.01 ng ml <sup>-1</sup>	24
LC-based sensor	Polarizing microscopy	0.001 ng ml <sup>-1</sup>	This work

**Fig. 6** POM images of LC cells with 5CB with different concentrations of cTnI without anti-cTnI: (a) 1 mg ml<sup>-1</sup>; (b) 0.1 mg ml<sup>-1</sup>; (c) 0.01 mg ml<sup>-1</sup>; (d) 0.001 mg ml<sup>-1</sup>.**Fig. 7** POM images of LC cells with 5CB with different proteins: (a) 1 μg ml<sup>-1</sup> IgG; (b) 1 μg ml<sup>-1</sup> ALB; (c) PBS buffer; (d) 1 μg ml<sup>-1</sup> cTnI.

### 3.5 Specificity

In addition to sensitivity, selectivity and specificity are also of great importance for detecting cTnI among various biomolecules in human plasma. The specificity of this LC-based immunosensor was assessed by measuring two types of non-specific proteins, namely IgG and ALB. These proteins and cTnI were diluted in PBS with the same concentration of 1 μg ml<sup>-1</sup>. Then, they were incubated on the DMOAP/APTES/GA/anti-cTnI-coated slides, and a series of LC cells were prepared. From the experimental results illustrated in Fig. 7, the biosensor responds differently to other proteins in contrast with cTnI. The optical image appeared bright when cTnI was incubated on the slides (Fig. 7d). On the contrary, the optical image appears almost all-dark when other proteins were decorated on the slides (Fig. 7a and b). There are a few bright spots in Fig. 7b due to the non-specific binding of the protein<sup>32</sup> or the tiny dust effect during the experiment. Meanwhile, we took the PBS buffer solution as the control group (Fig. 7c) and found that PBS had almost no effect on the experimental result. These results indicate that no biological binding event

occurred on the slides except for the incubation with cTnI, demonstrating its high specificity.

## 4. Conclusion

In conclusion, a novel LC immunosensor for detecting the cTnI antigen based on the special birefringence effect of LC molecules is established in this study. The sensor utilizes a DMOAP/APTES mixed silylation reagent to self-assemble sensitive membranes to modify the glass substrate, which induces the LC molecules to be arranged in an ordered space. The specific binding between the cTnI antigen and anti-cTnI can destroy the ordered LC molecule alignment on the surface of the substrate, thereby causing the change of the POM images to realize the detection of cTnI. The minimum detection limit of the LC biosensor was 1 pg ml<sup>-1</sup>. Different from the one-sided sensing LC cell, we used the double sides of the LC cell for sensing, which improved the sensitivity and detection range of the sensor greatly. Besides, we found that the sensor

showed good selectivity by IgG and ALB. The method was simple in operation and has high sensitivity and is expected to be popularized for the rapid detection of other biomolecules.

## Conflicts of interest

The author(s) declare that they have no competing interest.

## Funding

This work was financially supported by the National Science Foundation of China (Grant No. U1531102, 61107059, 61775212), and the Fundamental Research Funds for the Central Universities (HEUCF181116).

## References

- 1 M. V. Westfall, E. M. Rust and J. M. Metzger, *Proc. Natl. Acad. Sci. U. S. A.*, 1997, **94**, 5444–5449.
- 2 S. I. Yasuda, P. Coutu, S. Sadayappan, J. Robbins and J. M. Metzger, *Circ. Res.*, 2007, **101**, 377–386.
- 3 K. M. Eggers, L. Lind, H. Ahlstrom, T. Bjerner, C. E. Barbier, A. Larsson, P. Venge and B. Lindahl, *Eur. Heart J.*, 2008, **29**, 2252–2258.
- 4 J. L. Kim, *Circulation*, 2002, **106**, 2366–2371.
- 5 P. A. Kavsak, A. R. Macrae, M. J. Yerna and A. S. Jaffe, *Clin. Chem.*, 2009, **55**, 573–577.
- 6 S. Melanson, D. Morrow and P. Jarolim, *Am. J. Clin. Pathol.*, 2007, **128**, 282–286.
- 7 R. Labugger, L. Organ, C. Collier, D. Atar and J. E. Van Eyk, *Circulation*, 2000, **102**, 1221–1226.
- 8 T. Keller, T. Zeller, F. Ojeda, S. Tzikas, L. Lillpopp, C. Sinning, P. Wild, S. Genth-Zotz, A. Warnholtz, E. Giannitsis, M. Möckel, C. Bickel, D. Peetz, K. Lackner, S. Baldus, T. Münzel and S. Blankenberg, *JAMA, J. Am. Med. Assoc.*, 2011, **306**, 2684–2693.
- 9 B. Zethelius, N. Johnston and P. Venge, *Circulation*, 2006, **113**, 1071–1078.
- 10 T. B. Horwich, J. Patel, W. R. Maclellan and G. C. Fonarow, *Circulation*, 2003, **108**, 833.
- 11 N. J. Mehta, I. A. Khan, V. Gupta, K. Jani, R. M. Gowda and P. R. Smith, *Int. J. Cardiol.*, 2004, **95**, 0–17.
- 12 H. J. He, M. S. Lowenthal, K. D. Cole, D. Bunk and L. Wang, *Clin. Chim. Acta*, 2011, **412**, 0–111.
- 13 F. S. Apple and P. O. Collinson, *Clin. Chem.*, 2012, **58**, 54–61.
- 14 F. S. Apple, L. A. Pearce, S. W. Smith, J. M. Kaczmarek and M. M. Murakami, *Clin. Chem.*, 2009, **55**, 930–937.
- 15 Y. Li, X. Wang, L. Xu and X. Wen, *Lab. Med.*, 2014, **45**, 82–85.
- 16 X. Ji, R. Takahashi, Y. Hiura, G. Hirokawa, Y. Fukushima and N. Iwai, *Clin. Chem.*, 2009, **55**, 1944–1949.
- 17 I. H. Cho, E. H. Paek, Y. K. Kim, J. H. Kim and S. H. Paek, *Anal. Chim. Acta*, 2009, **632**, 247–255.
- 18 M. Imazio, B. Demichelis, E. Cecchi, R. Belli, A. Ghisio, M. Bobbio and R. Trincherio, *J. Am. Coll. Cardiol.*, 2003, **42**, 2144–2148.
- 19 W. Y. Wu, Z. P. Bian, W. Wang, W. Wang and J. J. Zhu, *Sens. Actuators, B*, 2010, **147**, 298–303.
- 20 J. Wu, D. M. Crokek, A. C. West and S. Banta, *Anal. Chem.*, 2010, **82**, 8235–8243.
- 21 J. Kiely, P. Hawkins, P. Wraith and R. Luxton, *IET Sci., Meas. Technol.*, 2007, **1**, 270–275.
- 22 J. F. Masson, L. Obando, S. Beaudoin and K. Booksh, *Talanta*, 2004, **62**, 865–870.
- 23 T. Liu, L. L. Liang, P. Xiao, L. P. Sun, Y. Y. Huang, Y. Ran, L. Jin and B. O. Guan, *Biosens. Bioelectron.*, 2018, **100**, 155–160.
- 24 D. Sandil, S. Srivastava, B. D. Malhotra, S. C. Sharma and N. K. Puri, *J. Alloys Compd.*, 2018, **763**, 102–110.
- 25 A. Hussain, A. S. Pina and A. C. A. Roque, *Biosens. Bioelectron.*, 2009, **25**, 1–8.
- 26 R. A. M. Hikmet and J. Lub, *Prog. Polym. Sci.*, 1996, **21**, 1165–1209.
- 27 S. Liao, Y. Qiao, W. Han, Z. Xie, Z. Wu, G. Shen and R. Yu, *Anal. Chem.*, 2012, **84**, 45–49.
- 28 J. Y. Du, Q. F. Jiang, X. C. Lu, L. C. Chen, Y. Zhang and X. L. Xiong, *Analyst*, 2019, **144**, 1761–1767.
- 29 Y. Wang, L. Zhao, A. Xu, L. Wang, L. Zhang, S. Liu, Y. Liu and H. Li, *Sens. Actuators, B*, 2018, **258**, 1090–1098.
- 30 S. Yang, C. Wu, H. Tan, Y. Wu, S. Liao, Z. Wu, G. Shen and R. Yu, *Anal. Chem.*, 2013, **85**, 14–18.
- 31 J. M. Brake and N. L. Abbott, *Langmuir*, 2007, **23**, 8497–8507.
- 32 Y. Wang, Q. Hu, T. Tian, Y. Gao and L. Yu, *Anal. Chim. Acta*, 2016, **937**, 119–126.